



## Fabrication and characterizations of high density Si<sub>3</sub>N<sub>4</sub> - ZrO<sub>2</sub> ceramics

Kamol TRAIpanya<sup>1,\*</sup>, Thanakorn WASANAPIARNPONG<sup>1,2</sup>, and Charusporn MONGKOLKACHIT<sup>3</sup>

<sup>1</sup> Department of Materials Science, Faculty of Science, Chulalongkorn University, Pathumwan, Bangkok 10330, Thailand

<sup>2</sup> Center of Excellence on Petrochemical and Materials Technology, Chulalongkorn University Research Building, Pathumwan, Bangkok 10330, Thailand

<sup>3</sup> National Metal and Materials Technology Center, National Science and Technology Development Agency, Khlong Luang, Pathumthani 12120, Thailand

\*Corresponding author e-mail: traipanya@hotmail.com

### Received date:

30 January 2023

### Revised date:

7 June 2023

### Accepted date:

23 June 2023

### Keywords:

Silicon nitride;

Zirconia;

Pressureless sintering;

Mechanical properties

### Abstract

Silicon nitride and zirconia were mixed with SiO<sub>2</sub>, MgO, Y<sub>2</sub>O<sub>3</sub> as sintering additives and pressureless sintered at 1650°C in N<sub>2</sub> atmosphere for 2 h. The XRD results showed α-Si<sub>3</sub>N<sub>4</sub> was partially transformed to β-Si<sub>3</sub>N<sub>4</sub> with 3:3:5 weight ratio of SiO<sub>2</sub> : MgO : Y<sub>2</sub>O<sub>3</sub>. However, at 5 wt% of ZrO<sub>2</sub> addition promoted phase transformation of α-Si<sub>3</sub>N<sub>4</sub> to β-Si<sub>3</sub>N<sub>4</sub> while 35 wt% of ZrO<sub>2</sub> completely transformed to β-Si<sub>3</sub>N<sub>4</sub> phase. Si<sub>3</sub>N<sub>4</sub> has a lower density than ZrO<sub>2</sub>, bulk density of samples increases in correlation with the amount of ZrO<sub>2</sub>. Because there was no difference in hardness and flexural strength between sintered Si<sub>3</sub>N<sub>4</sub> samples with hardness of 13.41 GPa and 648.13 MPa along with increasing ZrO<sub>2</sub> variation up to 55 wt%. Furthermore, with 75 wt% ZrO<sub>2</sub>, the hardness was reduced to 10.57 GPa and the flexural strength decreased to 208.16 MPa. SEM images of Si<sub>3</sub>N<sub>4</sub> samples demonstrated the dense microstructure and 5 wt% ZrO<sub>2</sub> showed homogeneous ZrO<sub>2</sub> distributed among the Si<sub>3</sub>N<sub>4</sub> grains. As a result, the hexagonal rod-like form of β-Si<sub>3</sub>N<sub>4</sub> is clearly visible in 75 wt% ZrO<sub>2</sub>. Therefore, Si<sub>3</sub>N<sub>4</sub> with ZrO<sub>2</sub> can be sintered with the homogeneous microstructure of the α-Si<sub>3</sub>N<sub>4</sub> to β-Si<sub>3</sub>N<sub>4</sub> transformation and tolerable mechanical properties vary with ZrO<sub>2</sub> content.

## 1. Introduction

Silicon nitride (Si<sub>3</sub>N<sub>4</sub>) and zirconia (ZrO<sub>2</sub>) ceramics have been highly accepted for use in structural applications due to their high fracture toughness, hardness, strength, chemical inertness, high temperature stability, wear resistance, low coefficient of friction, and biocompatibility. Currently, Si<sub>3</sub>N<sub>4</sub> ceramics are one of the most used groups of high thermal application and processing, especially nozzles, valves, cutting tools, turbochargers, heater sheaths, abrasive material, and metallurgical casting and machining in general [1,2]. However, sintered silicon nitride by conventional sintering had failed due to primarily problem of the low interatomic diffusion ability and the high temperature dissociation of Si<sub>3</sub>N<sub>4</sub>, which resulted in microstructural coarsening [3]. Nowadays, it is well known that Si<sub>3</sub>N<sub>4</sub> was manufactured using the nitridation mechanism from packed of silicon powder or sintered with various additives in high nitrogen pressure. Accordingly, several sintering aids such as yttria, magnesia, and alumina must be added to reduce the sintering temperature via the liquid-phase mechanism. During sintering, the smaller powders of alpha phase begin to dissolve with the liquid phase and recrystallize into a beta phase with a hexagonal needle shape and grain growth with traces. Due to the fact that the process of transformation from α-Si<sub>3</sub>N<sub>4</sub> to β-Si<sub>3</sub>N<sub>4</sub> is irreversible mechanism. Then, there have been no reports on sintered material mechanical properties testing between alpha

phase and beta phase for comparative purposes. A glassy phase exists between the grain boundaries, resulting in a higher density [4]. Moreover, the high nitrogen pressure atmosphere is required to prevent the mass loss of Si<sub>3</sub>N<sub>4</sub>. Mitomo *et al.*, in 1977, discovered the Si<sub>3</sub>N<sub>4</sub> with 90% density was obtained by using packing powder with 1 MPa of nitrogen pressure. Subsequently, Giachello *et al.* demonstrated that high nitrogen pressure could be avoided by using compacted Si<sub>3</sub>N<sub>4</sub> powder containing MgO as a sintering additive embedded in Si<sub>3</sub>N<sub>4</sub> powder [5]. In 2006, Wasanapiarnpong *et al.* found that the Si<sub>3</sub>N<sub>4</sub> ceramics powder with SiO<sub>2</sub>-MgO-Y<sub>2</sub>O<sub>3</sub> as sintering additive were successfully sintered with high degree of alpha to beta phase transformation at 1600°C to 1750°C in 1 atm of N<sub>2</sub> atmosphere without packing powder [6].

For the zirconia (ZrO<sub>2</sub>) has been utilized in various commercial products in the field such as seal, pump and milling media [7]. In the past, pure ZrO<sub>2</sub> is difficult to sintering because restriction of phase transformation from tetragonal to monoclinic at 950°C on cooling resulting in 4% of volume expansion. This change in shape of volume transformation can result in catastrophic fracture and structural inconsistency [8]. Presently, stabilized zirconia with many oxides such as Y<sub>2</sub>O<sub>3</sub>, MgO, CeO<sub>2</sub> etc. could be eliminated effect from phase transformation especially when yttria was added into zirconia has two important effects. It broadens the range of the tetragonal phase field and lowers the temperature at which the tetragonal-monoclinic transformation occurs. From the excellent property about stress induce

transformation toughening mechanism of zirconia is widely accepted that led zirconia used as reinforcing in ceramic composite. The most dominant are alumina-zirconia composites, which outperform conventional alumina in terms of strength, toughness, and wear resistance. Recently, zirconia-based nanocomposites for biomedical applications as dental implants, hip joint have been developed with linking several toughening mechanisms such as tetragonal-monoclinic transformation, microcracking, and crack deviation due to the secondary phases. During the past decade  $\text{Si}_3\text{N}_4$  and  $\text{ZrO}_2$  have been studied in the different sintering atmosphere. However, a recent study was attempted to develop  $\text{Si}_3\text{N}_4$  composite materials utilizing  $\text{ZrO}_2$  as a reinforcement phase. Although the use of tetragonal zirconia as a reinforcement phase can effectively improve the fracture toughness of  $\text{Si}_3\text{N}_4$  ceramics, the well-known high-temperature interaction between the  $\text{ZrO}_2$  component and the  $\text{Si}_3\text{N}_4$  matrix has been frequently observed during sintering at temperatures above  $1600^\circ\text{C}$ , resulting in the formation of deleterious  $\text{ZrN}$  or  $\text{ZrON}$  phases [9].

Therefore, this study purposed on extensive various composition between  $\text{Si}_3\text{N}_4$ - $\text{ZrO}_2$  materials with sintering additives in unique sintering atmospheres and without packing powder by investigated on phase, density, hardness, flexural strength and microstructure after nitrogen gas pressureless sintering.

## 2. Materials and experimental

The raw materials used were various compositions of high purity  $\alpha$ - $\text{Si}_3\text{N}_4$  powders (SN E-10 grade, Ube Industries Ltd., Tokyo, Japan) and 3 mol%  $\text{Y}_2\text{O}_3$  stabilized  $\text{ZrO}_2$  powders (Inframmat, Advanced Materials) at 5, 35, 55 and 75 wt% with  $\text{SiO}_2$  (KE-P30, Nippon Shokubai Co. Ltd., Osaka, Japan),  $\text{MgO}$  (MJ-30, Iwatani Corp., Tokyo, Japan), and  $\text{Y}_2\text{O}_3$  (RU, Shin-Etsu Chemical Co. Ltd., Tokyo, Japan) as sintering additives by weight ratio of  $\text{SiO}_2 : \text{MgO} : \text{Y}_2\text{O}_3$  at 3:3:5 was shown in Table 1. Then the starting material powders were mixed by ball milling in a high-density polyethylene bottle (HDPE) with  $\text{Si}_3\text{N}_4$  ball in 99.9% ethanol for 24 h. The slurry was dried to powder in a rotary evaporator at  $60^\circ\text{C}$  through a 100-mesh screening sieve. The powders were uniaxially pressed at 25 MPa and cold isostatic press at 250 MPa for 5 min. The pellets were sintered at  $1650^\circ\text{C}$  for 2 h in a nitrogen atmosphere of 0.1 MPa. All sintered samples were measured for bulk densities using the Archimedes method. Phase compositions were determined by X-ray diffraction (D8-Advance, Bruker Corp., Billerica, MA, USA) with  $\text{Cu-K}\alpha$  radiation. The hardness values of the sintered materials were prepared by grinding and polishing, then measured using Vickers hardness indentation at 10 kN for 15 s. Finally, polished surface of samples was chemically etched with HF

for 15 s for the microstructure observation using a scanning electron microscope (JSM 6480LV, JEOL Ltd., Tokyo, Japan).

## 3. Results and discussion

### 3.1 Phases composition

Figure 1 indicates the XRD patterns of the SN, 5Zr, 35Zr, 55Zr, 75Zr, and Zr samples. It shows that the  $\text{Si}_3\text{N}_4$  (SN) sample contains both  $\beta$ - $\text{Si}_3\text{N}_4$  and  $\alpha$ - $\text{Si}_3\text{N}_4$  as the main phases has already occurred at  $1650^\circ\text{C}$  with  $\text{SiO}_2$ ,  $\text{MgO}$ , and  $\text{Y}_2\text{O}_3$  as sintering additives. The  $\text{SiO}_2$ - $\text{MgO}$ - $\text{Y}_2\text{O}_3$  system has an eutectic temperature about  $1400^\circ\text{C}$  that liquid phase sintering can be performed to achieve high densification at  $1650^\circ\text{C}$  for 0.1 MPa in  $\text{N}_2$  without packing powder [6,10].

Considering the peak height of the first three peaks compared between beta and alpha silicon nitride phases to estimate the proportions of the two phases, it was found that in the SN sample, the beta phase was about 70% and the alpha was about 30%. While the 5Zr sample was found to contain 83% beta, 12% alpha. It can be seen that the addition of 5 wt% of  $\text{ZrO}_2$  promotes the  $\alpha$  to  $\beta$  phase transformation, which is consistent with the research of H. Hyuga *et al.* [11]. While adding 35 wt% of  $\text{ZrO}_2$ , only  $\beta$ - $\text{Si}_3\text{N}_4$  and tetragonal zirconia ( $t$ - $\text{ZrO}_2$ ) phases were found. No  $\alpha$ - $\text{Si}_3\text{N}_4$  phase was found indicating that the addition of 35 wt% of  $\text{ZrO}_2$  completes the phase transformation. For the Zr sample, the sample contained single-phase tetragonal zirconia that confirmed the absence of the effect of sintering in the nitrogen atmosphere.

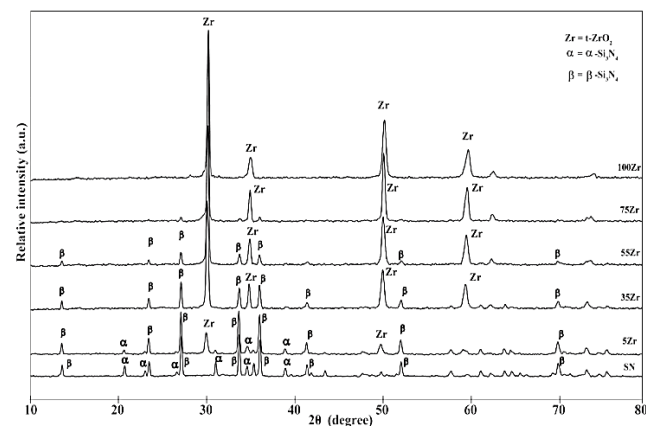


**Figure 1.** XRD patterns of  $\text{Si}_3\text{N}_4$  (SN), 5 wt%  $\text{ZrO}_2$  (5Zr), 35 wt%  $\text{ZrO}_2$  (35Zr), 55 wt%  $\text{ZrO}_2$  (55Zr), 75 wt%  $\text{ZrO}_2$  (75Zr),  $\text{ZrO}_2$  (Zr) samples sintering at  $1650^\circ\text{C}$  for 2 h.

**Table 1.** Starting materials with various composition.

Composition	SN	5Zr	35Zr	55Zr	75Zr	Zr
$\text{Si}_3\text{N}_4$	89	84	54	34	14	-
$\text{SiO}_2$	3	3	3	3	3	-
$\text{MgO}$	3	3	3	3	3	-
$\text{Y}_2\text{O}_3$	5	5	5	5	5	-
$\text{ZrO}_2$	-	5	35	55	75	100
Total	100	100	100	100	100	100

### 3.2 Density and water absorption

For the bulk density and relative density in Table 2. shows the changes in the bulk density, and relative density of the  $\text{Si}_3\text{N}_4$ - $\text{ZrO}_2$  composite ceramic samples SN, 5Zr, 35Zr, 55Zr, 75Zr, and Zr, respectively. With an increase in the  $\text{ZrO}_2$  content of the raw material, it can be seen that the bulk density of the samples increased relatively. The  $\text{Si}_3\text{N}_4$  (SN) samples have a density of about  $3.18 \text{ g}\cdot\text{cm}^{-3}$  and the 5Zr samples have  $3.28 \text{ g}\cdot\text{cm}^{-3}$  where the bulk density increases related to the amount of  $\text{ZrO}_2$  due to the density of  $\text{ZrO}_2$  being higher than that of the  $\text{Si}_3\text{N}_4$  materials. Furthermore, Zr samples have a density of  $6.05 \text{ g}\cdot\text{cm}^{-3}$  close to normal sintered  $\text{ZrO}_2$  that shows no effect of the ambient pressure  $\text{N}_2$  for  $\text{ZrO}_2$  and the XRD results demonstrated t- $\text{ZrO}_2$  without any ZrN formation. The bulk density of sintered samples was contrasted with relative density since the bulk density shows an increasing trend with amount of  $\text{ZrO}_2$  while the relative density reveals the effect of sintering additives. For SN, 5Zr, 35Zr, 55Zr, 75Zr and Zr samples have 98.70, 99.30, 99.15, 98.50, 97.20, and 99.18% relative density, respectively, with the relative density higher than 95% relative density shows that the  $\text{SiO}_2$ - $\text{MgO}$ - $\text{Y}_2\text{O}_3$  additive suitable plays the role in the approval of the sinterability of the samples.

### 3.3 Mechanical properties

Figure 2 Show the mechanical properties between Vickers hardness and flexural strength of all sintered samples as a role of  $\text{ZrO}_2$  content. The hardness decreased with increasing amount of  $\text{ZrO}_2$ . The inappreciably decrease in porosity of the samples may be related to the slightly dropped in hardness. A similar pattern emerged in the results of the flexural strength test. The SN samples exhibited higher hardness value when compared with a higher  $\text{ZrO}_2$  content. It can be seen that the hardness value of samples with 5 wt% to 75 wt% of  $\text{ZrO}_2$  decreases from 13.34 GPa to 10.57 GPa with increasing of the zirconia. It is widely known that the intrinsic property of the material has a significant impact on the hardness of dense multiphase ceramics because the hardness of  $\text{Si}_3\text{N}_4$  is mostly higher than the hardness of  $\text{ZrO}_2$ . According to reports, the hardness values of ceramics made of TZP,  $\alpha$ - $\text{Si}_3\text{N}_4$ , and  $\beta$ - $\text{Si}_3\text{N}_4$  are respectively between 11 GPa and 13 GPa, 23 GPa, and 20 GPa [12,13].

Additionally, we should be considered how  $\alpha$ - $\text{Si}_3\text{N}_4$  transform to  $\beta$ - $\text{Si}_3\text{N}_4$  during sintering because the significant partial portion of alpha phase dissolve by  $\text{SiO}_2$ - $\text{MgO}$ - $\text{Y}_2\text{O}_3$  liquid phase system and change to the beta phase was mainly referred by the phase transformation for the sample containing higher amounts of stablized  $\text{ZrO}_2$ . As a result,

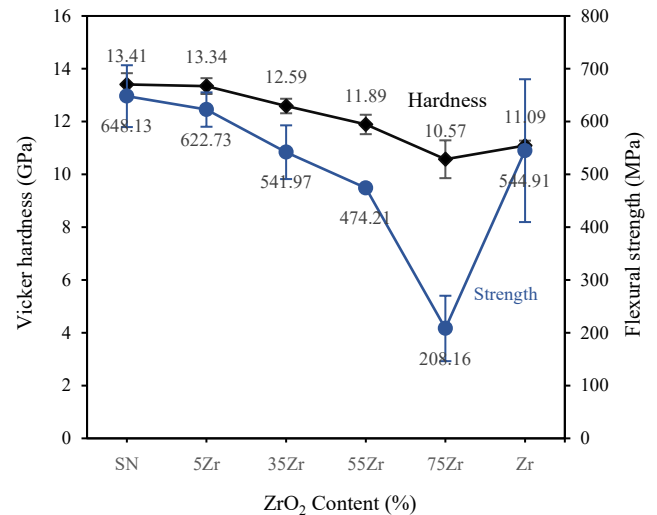


Figure 2. Vickers hardness and flexural strength of sintered  $\text{Si}_3\text{N}_4$ - $\text{ZrO}_2$  ceramics

the accelerated modification of alpha to beta may also subsidize to the recognized hardness decreasing in  $\text{Si}_3\text{N}_4$ - $\text{ZrO}_2$  ceramics [14]. The coincidental trend of the flexural strengths with hardness has shown a high value of 648.13 MPa for the SN sample particularly results from the achievement of a 98.43% relative density and a slightly decrease to 622.73 MPa for 5Zr by increasing the amount of  $\text{ZrO}_2$ . With regard, the increment of porosity results in the low flexural strength falling from 541.97 MPa for 35Zr, 474.21 for 55Zr, and 208.16 MPa for 75Zr respectively. Although the porosity of the Zr sample is not different from that of another sample but high strength because it exhibits a monolithic  $\text{ZrO}_2$ .

### 3.4 Microstructure

Figure 3 shows the SEM micrographs of the sintered samples with polished surface. SN sample with  $\text{SiO}_2$ ,  $\text{MgO}$  and  $\text{Y}_2\text{O}_3$  as sintering additive and Zr sample, the microstructure becomes homogeneous, dense, and low porosity correlate with high relative density and good mechanical properties.

However, in Figure 3(b), the microstructure of the 5Zr sample is remain uniform with light area of the  $\text{ZrO}_2$  grain in their microstructure. According to the results, the grain growth mechanism of the elongated  $\beta$ - $\text{Si}_3\text{N}_4$  grains is derived from the phase transformation mechanism and the added  $\text{ZrO}_2$  can promote  $\alpha$  to  $\beta$  phase transformation [15]. Also, by  $\text{ZrO}_2$  addition, complete phase transformation of  $\alpha$  to  $\beta$  through liquid phase sintering leads to  $\beta$ - $\text{Si}_3\text{N}_4$  hexagonal rod-like grains formation clearly in the 75Zr sample in agreement with XRD results.

Table 2. Bulk density, relative density, apparent porosity, and water absorption of sintered sample at  $1650^\circ\text{C}$  for 2 h under 0.1 MPa  $\text{N}_2$ .

Samples	SN	5Zr	35Zr	55Zr	75Zr	Zr
Bulk density ( $\text{g}\cdot\text{cm}^{-3}$ )	3.18	3.28	3.84	4.31	4.89	6.05
Theoretical density ( $\text{g}\cdot\text{cm}^{-3}$ )	3.22	3.30	3.87	4.38	5.03	6.10
Relative density (%)	98.70	99.30	99.15	98.50	97.20	99.18
Apparent density ( $\text{g}\cdot\text{cm}^{-3}$ )	3.18	3.28	3.85	4.32	4.90	6.06
Apparent porosity (%)	0.13	0.11	0.26	0.15	0.30	0.18
Water absorption (%)	0.04	0.03	0.07	0.04	0.06	0.03

\*3 samples/test

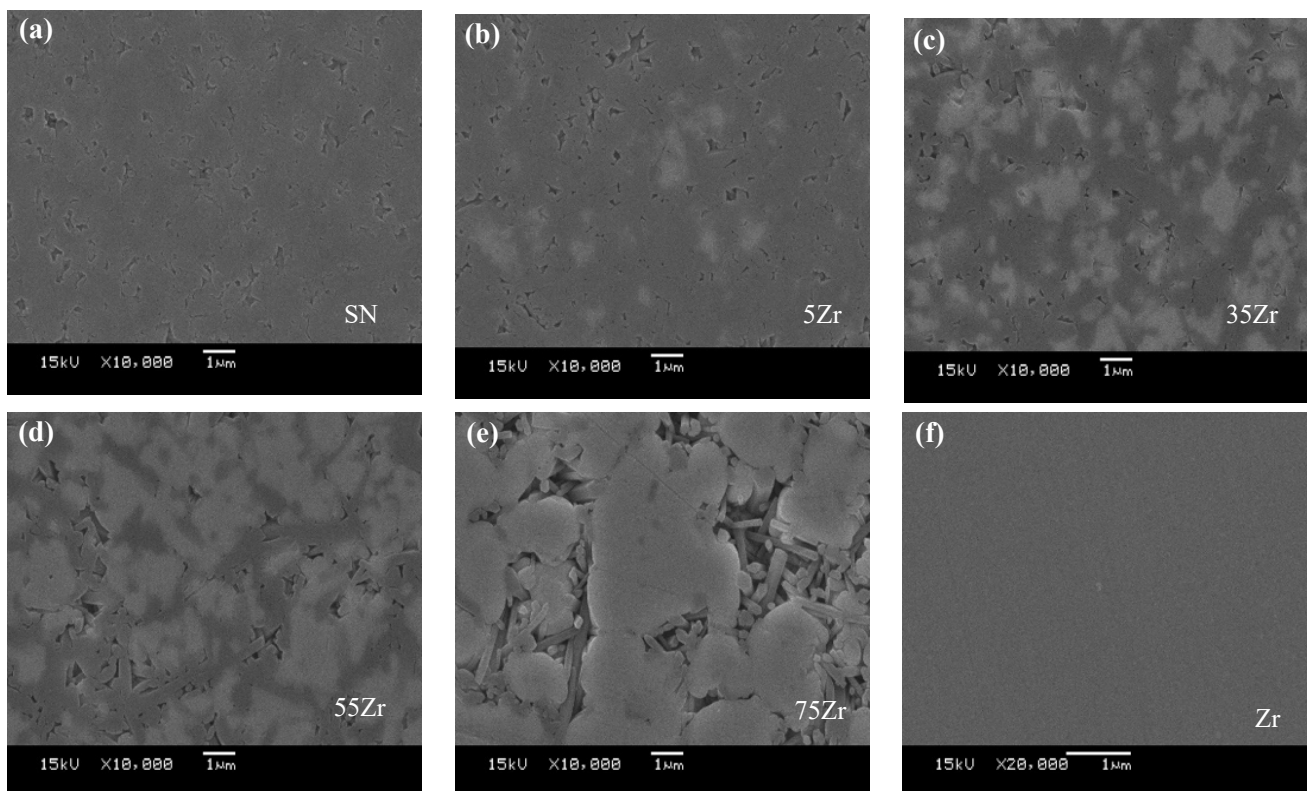


**Figure 3.** SEM micrographs of (a)  $\text{Si}_3\text{N}_4$  (SN), (b) 5 wt%  $\text{ZrO}_2$  (5Zr), (c) 35 wt%  $\text{ZrO}_2$  (35Zr), (d) 55 wt%  $\text{ZrO}_2$  (55Zr), (e) 75 wt%  $\text{ZrO}_2$  (75Zr), (f)  $\text{ZrO}_2$  (Zr) samples sintered at 1650°C for 2 h.

#### 4. Conclusions

Silicon nitride and zirconia were mixed with  $\text{SiO}_2$ ,  $\text{MgO}$ ,  $\text{Y}_2\text{O}_3$  and then pressureless sintering. According to the XRD results, the starting powders of  $\alpha\text{-Si}_3\text{N}_4$  were partially transformed to  $\beta\text{-Si}_3\text{N}_4$  with 3:3:5 weight ratio of  $\text{SiO}_2$  :  $\text{MgO}$  :  $\text{Y}_2\text{O}_3$ , respectively. At 5 wt% of  $\text{ZrO}_2$  was performed phase transformation of  $\alpha\text{-Si}_3\text{N}_4$  to  $\beta\text{-Si}_3\text{N}_4$  while 35 wt% of  $\text{ZrO}_2$  effectively transformed to  $\beta\text{-Si}_3\text{N}_4$  phase. The bulk density of the samples increases directly with the amount of  $\text{ZrO}_2$ . The hardness and flexural strength between sintered samples with high hardness of 13.41 GPa and 648.13 MPa along with increasing  $\text{ZrO}_2$  variation up to 55 wt%. But 75 wt%  $\text{ZrO}_2$ , the hardness decreased to 10.57 GPa and the flexural strength reduced to 208.16 MPa. SEM microstructures were presented, which showed a dense and homogeneous  $\text{ZrO}_2$  dispersion between  $\text{Si}_3\text{N}_4$  grains of 5 wt% of  $\text{ZrO}_2$  corresponding with the hexagonal rod-like of  $\beta\text{-Si}_3\text{N}_4$  is evidently at 75 wt%  $\text{ZrO}_2$ . From a distinctively sintering atmosphere,  $\text{Si}_3\text{N}_4$  and  $\text{ZrO}_2$  could be sintered together with uniform microstructure and mechanical properties acceptable.

#### References

- [1] Z. Krstic, and V. D. Krstic, "Silicon nitride: the engineering material of the future," *Journal of Materials Science*, vol. 47, pp. 535-552, 2012.
- [2] F. L. Riley, "Silicon nitride and related materials," *Journal of the American Ceramic Society*, vol. 83, pp. 245-265, 2000.
- [3] C. Greskovich, and J. H. Rosolowski, "Sintering of covalent solids," *Journal of the American Ceramic Society*, vol. 59, pp. 336-343, 1976.
- [4] G. G. Deeley, J. M. Herbert, and N. C. Moore, "Dense silicon nitride," *Powder Metallurgy*, vol. 4, pp. 145-151, 1961.
- [5] M. Mitomo, "Pressure sintering of  $\text{Si}_3\text{N}_4$ ," *Journal of Materials Science*, vol. 11, pp. 1103-1107, 1976.
- [6] T. Wasanapiarnpong, S. Wada, M. Imai, and T. Yano, "Lower temperature pressureless sintering of  $\text{Si}_3\text{N}_4$  ceramics using  $\text{SiO}_2\text{-MgO-Y}_2\text{O}_3$  additives without packing powder," *Journal of The Ceramic Society of Japan*, vol. 114, pp. 733-738, 2006.
- [7] A. Leriche, F. Cambier, and H. Reveron, "Zirconia ceramics, structure and properties," *Encyclopedia of Materials: Technical Ceramics and Glasses*, vol. 2, pp. 93-104, 2021.
- [8] R. H. J. Hannink, P. M. Kelly, and B. C. Muddle, "Transformation toughening in zirconia containing ceramics," *Journal of the American Ceramic Society*, vol. 83, pp. 461-487, 2000.
- [9] S. H. Ahmad, S. M. Rafiaei, S. Ghadami, and K. A. Nekouee, "Densification and mechanical properties of spark plasma sintered  $\text{Si}_3\text{N}_4/\text{ZrO}_2$  nanocomposites," *Journal of Alloys and Compounds*, vol. 776, pp. 798-806, 2019.
- [10] S. Kuang, M. J. Hoffmann, H. L. Lukas, and G. Petzow, "Experimental study and thermodynamic calculation of  $\text{MgO-Y}_2\text{O}_3\text{-SiO}_2$  system," *Key Engineering Materials*, vol. 89-91, pp. 399-404, 1994.
- [11] H. Hyuga, K. Yoshida, N. Kondo, H. Kita, J. Sugai, H. Okano, and J. Tsuchida, "Nitridation enhancing effect of  $\text{ZrO}_2$  on silicon powder," *Materials Letters*, vol. 62, pp. 3475-3477, 2008.

- [12] I. Hussainova, N. Voltsihhin, E. Cura, and S. P. Hannula, "Densification and characterization of spark plasma sintered ZrC– $\text{ZrO}_2$  composites," *Materials Science and Engineering: A*, vol. 597, pp. 75-81, 2014.
- [13] P. G. Hua, L. X. Guo, L. Min, L. Z. Hua, L. Qian, and L. W. Ian, "Spark plasma sintered high hardness  $\alpha/\beta$   $\text{Si}_3\text{N}_4$  composites with  $\text{MgSiN}_2$  as additives," *Scripta Materialia*, vol. 61, pp. 347-350, 2009.
- [14] P. Reis, J. P. Davim, X. Xu, and J. M. F. Ferriera, "Tribological behaviour of colloidally processed sialon ceramics sliding against steel under dry conditions," *Tribology Letters*, vol. 18, pp. 295-301, 2005.
- [15] K. Jeong, J. Tatami, M. Iijima, and T. Nishimura, "Spark plasma sintering of silicon nitride using nanocomposite particles," *Advanced Powder Technology*, vol. 28, pp. 37-42, 2017.